DEVELOPMENT OF A CMOS SNAPSHOT ACTIVE PIXEL SENSOR FOR SPACEBORNE EARTH OBSERVATION APPLICATIONS

Alex MATERNE, Christian BUIL

Centre National d'Etudes Spatiales, 18 Av Edouard Belin 31401 Toulouse Cedex 9.

ABSTRACT : *For metric resolutions earth observation missions – in the visible spectrum – CMOS Active Pixel Sensors (APS) may be a competitive alternative to 2D arrays CCD thanks to the high readout frequencies and to the shutter capability offered by the snapshot mode. In order to evaluate the interest of CMOS APS for those missions, CNES has launched the development of a CMOS snapshot APS demonstrator. Although a multi-mission capability is targeted, the requirement specification has been mainly built on the basis of a typical LEO micro-satellite mission scenario aiming at capturing images at 1 meter spatial resolution for a 8 km x 8 km minimum FOV, in the visible spectral band. Main driving requirements are presented together with the expected trade-off to be solved during architecture and design phases.*

1 - INTRODUCTION

Since the launch of SPOT-1 in February 1986, Earth surface imagers developed at CNES have been based upon the principle of linear scanning detectors – the so-called "pushbroom" principle – operating from a LEO polar heliosynchronous orbit.

The detection architecture takes benefits from the linear motion of the satellite to build a two-dimension image with a linear array detector.
The temporal axis given by the velocity direction is though conveniently employed but also completely monopolized by the building of one spatial axis.

The first detectors of the SPOT family were linear CCD arrays of photodiodes, with high photoresponse. However radiometric performances remain limited by the pushbroom constraints which restrict the integration time. Furthermore the scanning effect has its own contribution to the degradation of the contrast figure of merit, or modulation transfer function, (MTF).

A significant breakthrough occurred with the Time-Delay Integration CCD (TDI). TDI are photogate CCD arrays, including N photosensitive lines that transfer the charges at the same speed that satellite motion, while integrating photons, giving rise to a lengthened integration time, N times the sampling duration. The signal to noise ratio is multiplied by $N^{1/2}$. The synchronicity between charge transfer and satellite motion, as long as it is maintained, cancels the MTF contributors due to the scanning motion.

Even if they look physically like 2D-arrays, TDI remain based upon a pushbroom principle.

Alternative solutions, with no scanning, on the basis of 2D-CCD arrays, have been considered several times, in order to get a true 2D instantaneous single-shot image, with the benefit of a significant reduction of the amount of geometric corrections to be performed. But they were not

Report Documentation Page

Form Approved
OMB No. 0704-0188

Public reporting burden for the collection of information is estimated to average 1 hour per response, including the time for reviewing instructions, searching existing data sources, gathering and maintaining the data needed, and completing and reviewing the collection of information. Send comments regarding this burden estimate or any other aspect of this collection of information, including suggestions for reducing this burden, to Washington Headquarters Services, Directorate for Information Operations and Reports, 1215 Jefferson Davis Highway, Suite 1204, Arlington VA 22202-4302. Respondents should be aware that notwithstanding any other provision of law, no person shall be subject to a penalty for failing to comply with a collection of information if it does not display a currently valid OMB control number.

1. REPORT DATE	2. REPORT TYPE	3. DATES COVERED
13 JUL 2005	**N/A**	**-**

4. TITLE AND SUBTITLE	5a. CONTRACT NUMBER
Development of a CMOS Snapshot Active Pixel Sensor for Spaceborne Earth Observation Applications	5b. GRANT NUMBER
	5c. PROGRAM ELEMENT NUMBER
6. AUTHOR(S)	5d. PROJECT NUMBER
	5e. TASK NUMBER
	5f. WORK UNIT NUMBER
7. PERFORMING ORGANIZATION NAME(S) AND ADDRESS(ES) **Centre National d'EtudesSpatiales, 18 Av Edouard Belin 31401 Toulouse Cedex 9.**	8. PERFORMING ORGANIZATION REPORT NUMBER
9. SPONSORING/MONITORING AGENCY NAME(S) AND ADDRESS(ES)	10. SPONSOR/MONITOR'S ACRONYM(S)
	11. SPONSOR/MONITOR'S REPORT NUMBER(S)

12. DISTRIBUTION/AVAILABILITY STATEMENT
Approved for public release, distribution unlimited

13. SUPPLEMENTARY NOTES
See also ADM001791, Potentially Disruptive Technologies and Their Impact in Space Programs Held in Marseille, France on 4-6 July 2005., The original document contains color images.

14. ABSTRACT

15. SUBJECT TERMS

16. SECURITY CLASSIFICATION OF:			17. LIMITATION OF ABSTRACT	18. NUMBER OF PAGES	19a. NAME OF RESPONSIBLE PERSON
a. REPORT	b. ABSTRACT	c. THIS PAGE			
unclassified	**unclassified**	**unclassified**	**UU**	**11**	

Standard Form 298 (Rev. 8-98)
Prescribed by ANSI Std Z39-18

further investigated. They need a mechanism for compensation of the satellite motion during image shot, and a shutter mechanism to prevent from illumination during image readout.

The conjunction of these two functions degrades the overall principle reliability. The reading time, often larger than the integration time, leads to high levels of darkness signal that damage radiometric performances. The architecture of the focal plane is complicated for large fields applications.

For all these reasons, the 2D single shot principle, has been restricted to specific applications where, for instance, the temporal axis is dedicated to an alternative function. The French satellite PARASOL, a CNES microsatellite launched on December 2004, is an example of such applications. In this case the temporal axis is used to explore the spectral domain : 15 narrow band filters and polarizers are placed in succession in front of the CCD 2D-array.

In the domain of Earth observation for high resolution and very high resolution, the supremacy of TDI CCD detectors is settled for several years, even more with the high photo-response achievable with the back-thinning technologies.

They present, however, some drawbacks :
- the offer for back-thinned TDI devices is not very large : only two manufacturers in Europe,

- the readout frequency is limited,

- they need high levels of bias supplies and high power consumption to implement charge transfer in the registers.

2 - SNAPSHOT CMOS IMAGING SENSORS

The emergence of CMOS imaging sensors (CIS), for a decade, has not yet modified the position of CCD sensors for high resolution applications.

However, the CIS technologies offer several interesting features that could compete with CCD in the field of medium resolution (i.e. metric resolution) :

- wide offer,
- high readout frequencies,
- low consumption,
- high level of integration of on-the-chip processing functions leading to the “smart sensor” concept.

If we complete these performances with the electronic shutter capability of the so-called “snapshot” CIS, it can be seen that the limitations, up to now identified on CCD 2D arrays technologies, are significantly reduced. On the basis of this new potential, it becomes worth to revisit the double trade-off between CCD and CMOS, and between 2D and linear arrays, for space remote mapping applications, especially for those applications where the instantaneous feature of the image is of interest.

In a snapshot sensor, all the elementary detectors of the 2D array begin and complete photon to electron conversion at the same time. Once integration time is completed, the photo-carriers are synchronously converted in volts in a memory node built in the pixel, for subsequent reading out. The memory node is protected against the photon flux[1]. The system is called electronic shutter because the photon flux during readout has no impact on the collected signal.

The lay-out of a memory node reduces the useful area for photon detection, hence reduces the device response, but it brings the benefit of a true 2D single shot image, that is not achievable with common CIS devices where the photon to electron conversion is performed sequentially, line by line, in the rolling shutter mode.

3 - FROM THE MISSION TO THE SENSOR TECHNICAL REQUIREMENTS

3.1 - UPPER LEVEL REQUIREMENTS

In order to evaluate the performances of 2D CMOS imaging sensors, we have launched the development of a snapshot prototype. This section describes the main principles leading to the specifications. They come from previous studies managed by CNES for the development of imaging instruments, on LEO micro-satellites, in large visible spectral band, targeting fields over 8 x 8 km2. These studies were involving side options such as stereoscopic imaging and multispectral imaging over 4 narrow spectral bands.

More recently, complementary studies for new designs of instruments have been started under CNES management, in two distinct directions :

- low cost, 1 meter resolution earth imager on a LEO micro-satellite for a minimum 12 x 12 km2 field of view,
- 20 to 200 m resolution spectro-imager, covering more than 10 narrow spectral bands from UV to infrared wavelengths, on a GEO satellite allowing high revisiting frequency for survey purposes, with S/N requirements up to 500.

Table I and II hereafter give a reference set of specifications for a 1m resolution imager LEO micro-satellite.

Mission requirements	**Min**	**Typical**	**Max**
Spatial resolution		1 m	
Swath width	8 km	12 km	20 km
Altitude	500 km		700 km
Spectral band	[470- 720] nm		[470 – 830] nm
Spectral radiance levels	L1= 10 W/m^2.sr.µm L2 = 90 W/m^2.sr.µm L4 = 320 W/m^2.sr.µm		L1= 10 W/m^2.sr.µm L2 =100 W/m^2.sr.µm L4 = 350 W/m^2.sr.µm

Table I. Main mission requirements. Min and max values are given for each parameter. Various missions may be defined by selecting parameters within these ranges.

It is then necessary to add the minimum constraints in terms of volume and pointing stability in order to maintain the design in the range of the micro-satellites family :

Satellite and instrument design constraints	**Min**	**Typical**	**Max**
Optics diameter	0.3 m		0.4 m
Pointing stability (low frequency)			100 µrad/s

Table II. Main satellite requirements.

The performances requested are usually split in radiometric performances (represented by the signal to noise ratio) and spatial resolution (represented by the MTF).

Performances	Spécifications
MTF at Nyquist frequency νq	> 0.10
Signal to noise S/N @ L2 radiance level	> 90
MTF(νq) x S/N(L2)	> 10

Table III : Image performances.

From this very basic mission, it is possible to estimate the feasibility of complementary missions such as continuous mapping along the track, stereoscopic imaging, or multispectral imaging.

3.2 - MAIN DRIVING REQUIREMENTS

This section reviews how the upper level requirements lead to the technical requirements applicable for the sensor. We identify the domains where CMOS technology brings significant breakthrough, and the performances for which further improvements are still necessary to fit space imagers needs.

3.2.1 - *Field of view – spatial resolution*

The couple (field of view/ spatial resolution) forces the sampling array size to a minimum of 8000 x 8000 dots. This requirement is a main driver for the design of the device and for the architecture of the focal plane. Most CIS devices are less than 2048 x 2048 pixels arrays. Larger arrays request photocomposition of the device during the photolithography step of fabrication. This technique, also called stitching, allows repetition of several subsections of the layout in order to manufacture large devices. Unfortunately stitching is not available on every CMOS foundry, so the specific request for large arrays significantly reduces the offer.

It remains possible to adapt the focal plane architecture to accept small devices, using butting techniques or architectures with staggered detectors (Fig.1). These architectures avoid the development of too large devices, for which manufacturing yields are often a source of concern. A good compromise starts from an already large array – about 4000 x 4000 – arranged in the focal plane to obtain fields from 8000 x 8000 to 20 000x 20 0000.

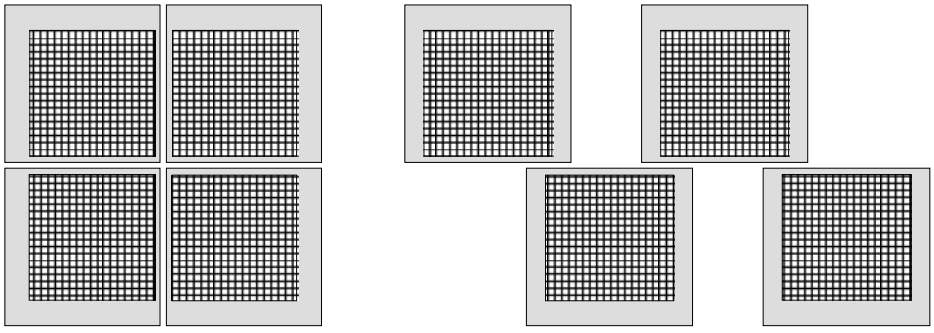

Figure 1 : 8kx8K focal plane architecture with 4 butted devices and 16Kx8K focal plane architecture with 4 staggered devices.

3.2.2 - *Timing*

The time allocated to the image shot, or integration time, is mainly limited by the low frequency drift of the pointing axis. We have considered a global performance better than 100 µrad/s, which is in the domain of feasibility for microsatellites stabilization units. We have also considered, in first approach, that this allocation includes the stability of the system in charge of motion compensation. The drift of the pointing axis during the integration time must be less than 0.25 times the ground sample distance, in order to ensure a MTF degradation less than about 2.5 %.

The maximum integration time allowed is then given by :

$$Ti = 0.25 \bullet \frac{gp}{H \bullet Stab} \qquad [1.]$$

where gp is the ground pitch, H is the altitude and Stab is the stability of the pointing axis.

That leads to 5 ms at an altitude of 500 km, and 3.5 ms at 700 km.

The time, Tr, allowed for readout is strongly linked to the size of the sampling array. For a 4000 x 4000 array, the time separating two successive fields along the track is 568 ms at 500 km. It requires a readout frequency of about 28 Mpix/s which is rather low, taking into account that frequencies up to hundred of Mpix/s can be achieved on CMOS 2D arrays.

It can be seen that the mission requirements are not demanding for this parameter of readout frequency. However, it is worth taking advantage of the high readout frequencies offered by the technology in order to, firstly, reduce the parasitic signal during readout, which behaves in first order like Tr, and secondly to multiply the operations implemented during one field coverage. It may be possible for instance to divide the arrays in 4 subsections 4000 x 1000 across the track with 4 different narrow band filters on the top, and thus to explore multiple spectral bands by repeated images every 142 ms. The limit of this approach will be dictated by the performances of the mechanism for motion compensation. Angular strokes within several milliradians during 3 to 5 millisecondes, with hundreds of milliseconds for repositioning do not present major problems. It may become critical when one search for larger strokes together with higher angular velocity for repositioning.

3.2.3 - *Shutter efficiency*

The relative parasitic responsivity γp is the ratio of the parasitic responsivity of the memory node to the useful responsivity of the pixel.

Let Su(L1) be the useful signal for a spectral radiance L1 for an integration time Ti, and Sp(L2) the parasitic signal received during readout Tr in the memory node, under a spectral radiance L2.

$$S_u(L_1) = R_u \bullet L_1 \bullet Ti \qquad [2.]$$

$$S_p(L_2) = R_p \bullet L_2 \bullet Tr \qquad [3.]$$

If we try to maintain Sp(L2) < 0.02 Su(L1), we get :

$$\gamma_p = \frac{R_p}{R_u} = 0.02 \bullet \frac{Ti}{Tr} \bullet \frac{L1}{L2} \qquad [4.]$$

Taking L1 = Qsat/30 et L2 = Qsat/3, gives :

$$\gamma_p = 2.10^{-3} \bullet \frac{Ti}{Tr} \qquad [5.]$$

Taking into account an architecture that privileges high readout frequencies, with Tr < 50 ms, leads to a specification $\gamma p = 8\ 10^{-5}$, for Ti = 2 ms, minimum.

This specification is very demanding. So, it appears necessary to investigates alternatives to relax it. It is possible, for instance, to maintain the motion compensation during readout in such a way that the same image is seen during readout. At the frontier between L1 and L2 landscapes, it is not possible to guarantee that the pointing axis will maintain the position of the image within the requested performance, but there is a probability that, for a fraction of the readout time, the parasitic signal collected squares with the useful signal.
In this case, the extra signal collected during readout becomes :

$$\frac{\Delta S}{S_u} = \gamma_p \bullet P(L1) \bullet \frac{Tr}{Ti} + \gamma_p \bullet P(L2) \bullet \frac{L2 \bullet Tr}{L1 \bullet Ti} = \frac{\Delta S_u}{S_u} + \frac{\Delta S_p}{S_u} \qquad [6.]$$

where P(L2)=1-P(L1) states for the probability to drift from the L1 scene to a L2 scene on the ground. The first contribution is in addition to the useful signal. The second one is a true parasitic signal : at the frontier between L1 and L2 scenes it will have the same effect as a diffusion MTF, negligible if the ratio is kept smaller than a percent of Su(L2) or 10% of Su(L1). As we consider pixels farther from the transition, P(L2) decreases, and ΔSp/Su decreases too. Table IV gives the performance γp for various system conditions.

ΔSp/Su	L2 W/(m2.sr.µm)	L1 W/(m2.sr.µm)	Tr ms	Ti ms	P(L2)	γp	Comment
2 %	100	10	50	2	1	8.10^{-5}	No compensation during readout
2%	100	10	50	2	0.5	$1.6\ 10^{-4}$	With compensation
2 %	100	10	50	5	0.5	4.10^{-4}	With extended integration time
10%	100	10	50	2	0.5	$8.\ 10^{-4}$	With relaxed objective

Table IV. System parameters for shutter efficiency optimization.

We shall use two levers in order to improve the shutter efficiency :

- at system upper level, via an architecture with high readout frequency,
- at pixel level, via a design optimized for shutter efficiency.

This optimization includes a trade-off between photoresponse and shutter efficiency.

3.2.4 - *Dynamic range*

The dynamic range is deduced from the requirements in spectral radiance range and S/N(L2) x FTM, taking into account the contribution expected from the system noise.

The S/N requirement, enhanced to meet the S/Nx FTM criteria, may be expressed in electrons by

$$Q(L2) / \sqrt{Q(L2) + B_{0\det}^2 + B_{sys}^2} = 100 \qquad [7.]$$

where the first term under square root stands for the photon shot noise, B0det is the noise of the device in darkness, Bsys is the system noise, each of them expressed in electrons. From the spectral radiance range, we will assume, Q(L2)min = Q(L4)max/4.

$$\frac{Q(L4)}{\sqrt{Q(L4)/4 + B_{0\det}^2 + B_{sys}^2}} = 400 \qquad [8.]$$

Q(L4)max deduced from the resolution of equation [8.] above gives the minimum charge storage capability Qsat min requested to achieve the S/N performance.

The darkness noise is deeply depending on the pixel architecture, on the implementation of correlated double sampling (CDS), and must include shot noise from charges thermally generated in darkness. For architectures without CDS, the kTC noise will dominate, and the contribution from the system noise may be considered negligible. Equation [8.] is now reduced to :

$$Q_{sat\,\min} = 2.10^4 \bullet (1 + \sqrt{1 + 4.10^{-4} \bullet B_{0\det}^2}) \qquad [9.]$$

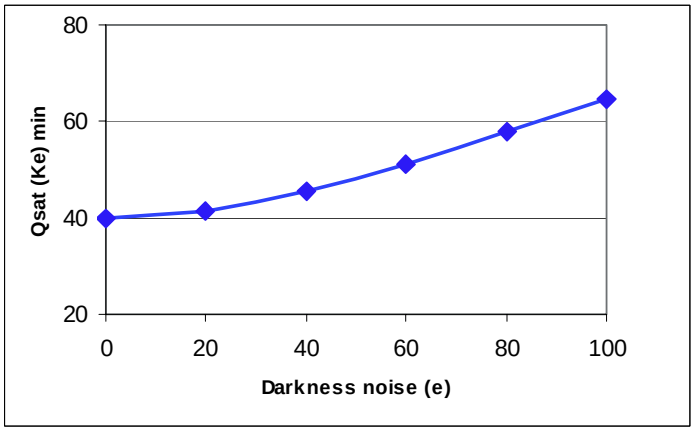

Figure 2. Minimum charge storage capacity requested as a function of darkness noise.

There is a threshold of charge handling capability that must exceed 40 Ke to take into account the photon shot noise. Besides, it appears relatively useless, for the Qsat optimization, to fight for darkness noise levels lower than about 40 e, as the slope dQ/dB_0 decreases.

3.2.5 - *Sensitivity*

For CMOS imaging sensor the main performance is given by the QE.FF of the pixel, where QE is the quantum efficiency and FF is the fill factor representing the ratio of the photosensitive area over the total area of the pixel. The performance needed for QE.FF may be derived from the equation hereafter :

$$Q(L4) = L4 \bullet QE \bullet FF \bullet \frac{\lambda}{hc} \bullet \Delta\lambda \bullet Ti \bullet \frac{\pi}{4} \bullet D^2 \bullet \left(\frac{p}{f}\right)^2 \bullet Ktel \qquad [10.]$$

where λ : mean wavelength, Δλ : spectral bandwidth, hc : 1,98 10^{-25} $J.m^{-1}$,Ti : integration time, D : optics diameter, p: pixel pitch, f : focal length, Ktel : telescope global transmission

Assuming that Q(L4) has to reach Qsatmin to meet S/N requirements, allows to determine a relationship between charge storage capability and QE.FF :

$$Q_{sat\,\min} = L4 \bullet QE \bullet FF \bullet \frac{\lambda}{hc} \bullet \Delta\lambda \bullet Ti \bullet \frac{\pi}{4} \bullet D^2 \bullet \left(\frac{gp}{H}\right)^2 \bullet Ktel \qquad [11.]$$

In this equation the ratio p/f has been substituted by gp/H where gp is the ground pitch and H is the altitude of the satellite. It follows that the pixel size is no more necessary to determine Qsat and QE.FF requested.

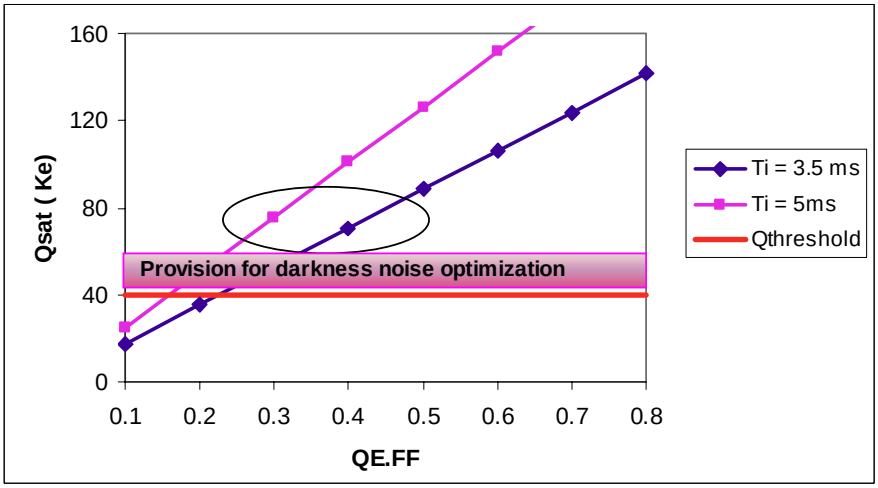

Figure 3. Example of relationship between Qsat and QE.FF, assuming H=600 km; D=0.3 m; KTel =0.7; Δλ=0.35µm ; λ=650 nm.

For a limited domain within the reference mission area, (see Figure 3), a 1m resolution mapping is achievable in spite of relatively low QE.FF. In this case the design and technology efforts may be directed towards higher shutter efficiencies, or smaller pixel sizes.

For most observation missions, more demanding in terms of response (narrower bands, higher altitude (fig.4), higher resolution) or more demanding in terms of signal to noise (GEO satellites), the QE.FF performance has to be improved up to the performance achieved with CCD photodiodes arrays, or even with back-illuminated CCD photogates.

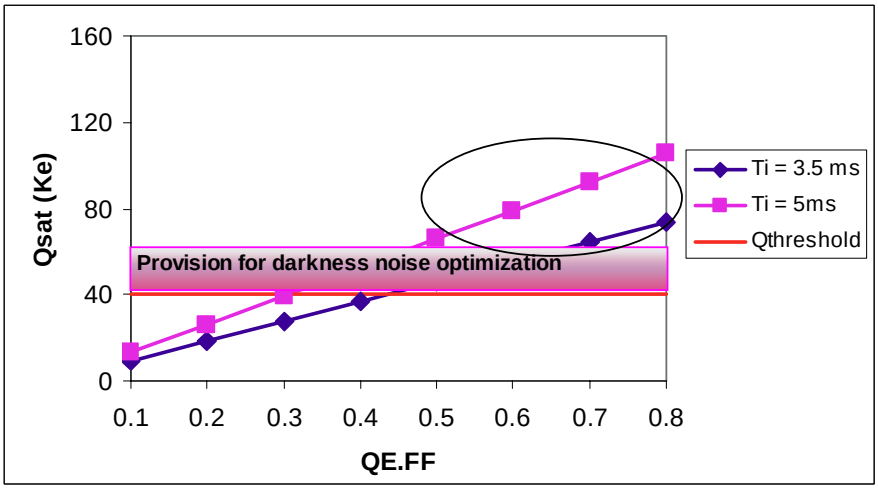

Figure 4. Relationship between Qsat and QE.FF, assuming H=700 km; D=0.3 m; KTel =0.7; Δλ=0.25µm ; λ=590 nm.

Such values appears to be hardly achievable in CMOS when it is requested to get them together with high shutter efficiency and large arrays.

Improvements must be investigated in the design and technology of the pixel, in several directions :

- via simplification of the stack of layers over the pixel aperture, or better optical transmission of these top layers[2].
- via better charge collection efficiency, in the pixel itself,
- via microlenses on the top of the die, as already performed by some foundries.
- via noise reduction, to reduce the Qsat min requested, which linearly impacts the QE.FF.

On the other hand, some alternatives may be investigated at system level, in order to get round the low response or dynamic range. A significant (in $N^{1/2}$) improvement in signal to noise may be achieved via summing up N times the same image. Such a principle can be explored, thanks to the capabilities offered by an architecture allowing :

- instantaneous 2D image shot, that will simplify image-to-image repositioning before summing up,
- high readout frequencies.

It should be more easily considered for GEO observation than for LEO observation. For LEO satellites, it remains strongly dependant on the motion compensation performances, because the critical requirements are displaced on the mechanism for which it is now requested to deal with angular strokes covering a time duration N.(Ti + Tr) instead of Ti.

3.2.6 - *MTF*

A contribution of 0,50 for the detector is in the domain of feasibility for the shorter wavelengths of the specified spectral band. It becomes more demanding in the vicinity of λ = 800 nm, as in most front illuminated CCD, due to the diffusion of photo-generated charges.

The reduction of the effective photosensitive area, due to the electronic functions located in the pixel and due to the memory node mask, induce a slight increase in geometric MTF, because the pixel width is smaller than the pixel pitch.

A major consequence of the MTF behaviour at longer wavelength may be a restriction of the spectral band that will finally increase the pressure for better QE performances, or a larger pixel size to reduce diffusion terms and get better QE.

3.2.7 - *Pixel pitch*

The large variety of elementary functions to be dealt with pushes toward a higher pixel size to include the shutter function without sacrificing the electro-optic performances. The counter part is a higher focal length, restricting the solutions to telescopes designs, such as Korsch type, that can manage large focal length in small volumes.

The pixel size limit is rather located at the focal plane. A large pixel size together with the large field of view specification creates constraints that become unsolvable when considering stereoscopic options.

On the other hand, the device manufacturing technologies have their own capabilities : state-of-the-art in CCD TDI photogate technology with 4 phases is located near 13 µm. In CMOS technology, the pixel size is in a continuous trend for shrinking. The powerful Moore's law is working for more and more integration. Integration means scaling down the main parameters of the design : as gate

length is reduced, thanks to advances in lithography processes, oxide thickness and voltages are reduced too. Pixel size less than 5 µm are available, from 0.18 µm foundries, but their electro-optic performances are slightly different from those one would obtained from a 0.5 µm foundry, because the scaling effects[3] have changed not only the surfaces dimensions but also the top layers topology, where optical effects occur, and the depletion depth where collection of photo-carriers takes place.

It sounds obvious then to specify the smaller pixel size achievable to meet QE.FF mimimum values above 0.25, that would lead us above 10 µm, and to put the upper barrier in the vicinity of 15 µm which would result in a focal plane maximum length of 0.3 m (for the 20 km swath width) at the same dimension as the optics diameter.

3.2.8 - *Synthesis of main requirements*

The table hereafter gives the limit of the domain of feasibility for the 1m resolution LEO mission considered in reference. An optimization of this set of performances is in progress, during the architecture phase. The basic trade-off include :
- balance between shutter efficiency and fill factor,
- balance between readout time and array dimensions,
- balance between fill factor and pixel size.

Parameter	**Min**	**Typ**	**Max**	**Comment**
QE.FF	0.25	0.4		
Qsat min (Ke)	75			
MTF @ Nyquist	0.50			
Noise in darkness (e)			70	
Pixel pitch (µm)		10	15	
Shutter efficiency			$8.\ 10^{-4}$	
Readout time (ms)			50	For a 4Kx4K array
Array size	2Kx2K	4Kx4K		

Table V. Main requirements.

The aim of this development is to demonstrate the capability for manufacturing a 4000 x 4000 sensor with the same set of masks. The specified readout frequencies should allow readout times less than 50 ms for the whole array, that contributes to the shutter efficiency and opens the road for summing up the images.

4 - DISCUSSION AND CONCLUSION

CMOS technologies make possible detection architectures that were previously rejected due to the limitations inherent to CCD capabilities. Higher readout frequencies associated with electronic shutter capabilities makes the snapshot 2D image more attractive with respect to the well-established pushbroom mode.

However, radiometric performances remain under the performances offered by the CCD technologies, especially for all high-resolution applications. Improvements are already going on in order to overcome these drawbacks, in multiple ways :

- through the spreading of the stitching offer,
- through the development of specific processes dedicated at better optical performances.

These processes exist. The big issue is to get them together with stitching on an available manufacturing line, interested in small volume applications. Most of manufacturing lines concentrate their development efforts in the direction of a higher integration, which remains the driver for cost reduction in the field of high volume applications. This general trend works properly for most electronic applications, and, up to now, electro-optic devices took advantage from the progress made for electronics.

But the commonality of interest between electronic and electro-optic applications does not work so easily when the design main dimensions become smaller compared to the wavelength of interest. In this case the device must be thought differently and the same processes cannot meet both the electronic and optic requirements.

The disruption in space applications will come with the cohabitation, in the pixel itself, of highly integrated CMOS electronic processes with dedicated imaging processes.

5 - BIBLIOGRAPHY

[1] 1024x1280 pixel dual shutter APS for industrial vision. Herman Witters, Tom Walschap, Guy Vanstraelen, Genis Chapinal, Guy Meynants, Bart Diedrickx. Presented at SPIE Electronic Imaging, Santa Clara, January 2003.

[2] Detection of visible photons in CCD and CMOS: a comparative view. P. Magnan. Nuclear Instrument and Methods in Physics research A 504 (2003) 199-212.

[3] Nanoscale CMOS. H.S.P. Wong, D.J. Frank, P.M. Solomon, C.H.J. Wann, J.J. Welser Proceedings of the IEEE, Vol 87, n°4, April 1999.